BŞEÜ Fen Bilimleri Dergisi
6. Cilt - Prof. Dr. Fuat SEZGİN Bilim Yılı Özel Sayısı
123-134, 2019

BSEU Journal of Science
DOI: 10.35193/bseufbd.577918

e-ISSN: 2458-7575 (http://dergipark.gov.tr/bseufbd)

Araştırma Makalesi / Research Article

Grafen Nanoparçacık Boyutunun Katkılı Faz Değişken Malzemelerin Termal Özelliklerine Etkisi

Size Effect of Graphene Nanoparticles on the Thermal Properties of the Doped Phase Change Materials

Ümit Nazlı Temel[1*], Eyüp Erdiş[2]

Geliş / Received: 13/06/2019 ***Revize / Revised: 03/09/2019*** ***Kabul / Accepted: 03/09/2019***

Öz- Bu çalışmada, parafin tipi bir organik Faz Değişken Malzeme (FDM) içerisine katkılanan Grafen nanoparçacık boyutunun termal özellikler üzerindeki etkileri incelenmiştir. Üç farklı boyuta sahip GNP nanoparçacıkların organik bir FDM içerisine %1, %3 ve %5 kütle bölüntülerinde katkılanması suretiyle elde edilen GNP/FDM kompozitlerinin ısıl iletkenlik, erime/katılaşma sıcaklıkları ve erime/katılaşma gizli ısıları ölçülmüştür. Termal özelliklerde elde edilen değişimler katkılanmamış FDM verileri referans alınarak belirlenmiştir. Elde edilen sonuçlar, düşük GNP kütle bölüntülerinde ısıl iletkenlik iyileştirmesinin hem GNP nanoparçacık yüzey alanının hem de kalınlığının bir fonksiyonu olduğunu göstermiştir. Buna ilave olarak, daha kalın nanoparçacıkların yüksek FDM kütle bölüntülerinde daha etkin bir iletim ağı oluşturdukları belirlenmiştir. Çalışmada ayrıca ısıl iletkenlikte elde edilen iyileştirmelerin termal performansa yansımaları da belirlenmiştir. GNP nanoparçacık kalınlığındaki artışa bağlı olarak ısıl iletkenlikteki iyileşmeler; 5% GNP(1-5nm)/ FDM, 5% GNP(6-8nm)/FDM ve 5% GNP(11-15nm)/FDM kompozitleri için sırasıyla %6.3, %107.5 ve %113.7 olarak elde edilmiştir. Bu ısıl iletkenlik iyileştirmeleri, bir enerji depolama biriminde sırasıyla %5.5,% 18.3 ve % 20 civarında performans artışı sağlamıştır.

Anahtar Kelimeler **- FDM, Isıl Iletkenlik, Boyut Etkisi, Grafen Nanoparçacık**

A*bstract-* **In this study, the size effects of the Graphene nanoparticles (GNP) doped into a paraffin type organic phase change material (PCM) on thermal properties were examined. The thermal conductivities, melting/solidification temperatures and melting/solidification latent heats of the GNP/PCM composites, which were obtained by incorporating GNP nanoparticles with three different sizes into an organic PCM in mass fractions of 1%, 3% and 5%, were measured. The changes obtained in thermal properties were determined by referring to the non-doped PCM data. The results obtained showed that in low PCM mass fractions, thermal conductivity enhancement was a function of both surface area and thickness of the GNP nanoparticles. In addition, it was determined that thicker nanoparticles formed a more efficient conduction network at high PCM fractions. The reflections of the enhancements obtained in thermal conductivity on thermal performance were also determined in the study. Enhancements in thermal conductivity depending on the increase in thickness of GNP were obtained as 6.3%, 107.5% and 113.7% for 5% GNP(1-5nm)/ PCM, 5% GNP(6-8nm)/PCM and 5% GNP(11-15nm)/PCM composites, respectively. These thermal conductivity enhancements resulted performance increase in the energy storage unit around 5.5%, 18.3% and 20% respectively.**

Keywords**- PCM, Thermal Conductivity, Size Effect, Graphene Nanoparticles**

[1]*Sorumlu yazar iletişim: untemel@cumhuriyet.edu.tr (https://orcid.org/0000-0001-5053-5124)
Department of Mechanical Engineering, Sivas Cumhuriyet University, Sivas, TURKEY
[2]İletişim: eyuperdis@hotmail.com (https://orcid.org/0000-0002-6643-0121)
Department of Energy Science and Technology, Sivas Cumhuriyet University, Sivas, TURKEY

I. INTRODUCTION

Phase change materials (PCMs) are energy storage materials that have a wide usage potential in engineering applications. Due to their high energy storage capability, they can be used in many engineering applications such as energy storage [1-3], active and passive cooling [4,5], and thermal protection of battery packs [6-8]. Paraffin based organic PCMs are the most preferred type of PCMs due to their advantages such as chemical-thermal stability, easy and economical attainability. However, the most important known drawback of this type of PCMs is that their thermal conductivity is low. Low thermal conductivity is directly associated with the speeds of energy storage/release of organic PCMs and it is the most important obstacle in their efficient use in practice.

The enhancement in thermal conductivity of PCMs for the more efficient usage in practice has been a point of interest for researchers in recent years. For this purpose, methods such as adding fins with high thermal conductivity in PCMs [9,10] or impregnating PCMs into the pores of metal foams with high thermal conductivity [11,12] were applied in prior studies conducted in the literature. Although these methods increase thermal conductivity significantly, they cause certain disadvantages such as limitation of the amount of PCM that can be used, increase in system weight/volume, low stability and crystallization. For increasing the thermal conductivities of PCMs, methods including adding nanoparticles into PCMs began to be used in recent years in order to overcome these negativities. The enhancements up to 26% in the thermal conductivities of metal/metal oxide nanoparticles doped PCMs [13,14] were not seen as sufficient. In their study in which they evaluated the effects of various types of nanoparticles on the thermal conductivity of PCMs, Temel and Çiftci [15] determined that carbon-based nanoparticles performed better compared to metal/metal oxide nanoparticles.

Carbon-based nanoparticles have low density and high thermal conductivity and they can be synthesized in the shape of the tube (MWCNTs), fiber (CNF) and plate (GNP). When the enhancements provided in the thermal conductivities of carbon-based nanoparticle doped PCMs in the literature are examined, it was seen that improvements of; i) between 24%-51.6% in the thermal conductivities of the MWCNT doped PCMs [16,17], ii) between 15%-44% in the thermal conductivities of the CNF doped PCMs, and iii) between 200%-400% in the GNP doped PCMs were provided [18,19]. In conclusion, it is clear that plate-formed carbon nanoparticles enhance the thermal conductivities of PCMs better. Although the carbon-based nanoparticles of different forms have the same bulk thermal conductivity, the superiority of GNP nanoparticles in enhancing PCM thermal conductivity can be explained as follows. The fact that the GNP nanoparticles are in the form of plates causes lower thermal resistance in the GNP/ PCM interface and a more suitable network structure for phonon scattering [20].

As can be seen from the studies conducted in the literature, the studies on the thermal enhancement of PCMs through adding carbon-based nanoparticles are mainly focused on nanoparticle shape and method difference. However, it is seen that no studies were carried on the size effect of GNP nanoparticle on thermal properties. Therefore, this study was focused to investigate the effects of different size properties for the same type of GNP nanoparticles on thermal properties. In the study, the reflections of the thermal conductivity enhancements of the obtained composites on performance were also determined with tests conducted in an energy storage unit.

II. MATERIAL AND METHOD

In the study, a paraffin-based organic phase change material (A82) with a melting peak temperature of 82 ^{o}C, commercially obtained from the company PCM Product (United Kingdom), was used as the energy storage material. The latent heat, density and specific heat of A82 is around 170 J/g, 800 kg/m^3 and 2.21 kJ/kgK respectively and its maximum operating temperature is about 250 ^{o}C. In order to enhance the thermal conductivity, Graphene nanoplatelet (GNP), which has different size properties, obtained from the company Skyspring Nanomaterials (USA) was used as the nano-filling material. The physical properties of the GNP nano-filling materials used in the study are given in Table 1.

Table 1. Physical Properties of GNP

	Nano-Filling Materials			
	Shape	**Thickness (nm)**	**Surface Area (m^2/g)**	**Purity (%)**
GNP (1-5 nm)	Plate	1-5	750	99.5
GNP (6-8 nm)	Plate	6-8	120-150	99.5
GNP (11-15 nm)	Plate	11-15	50-80	99.5

The GNP/A82 composites were prepared using a method that consists of melting and mixing. Firstly, a certain amount of solid A82 placed inside a glass container was heated on the heating plate until completely liquefied. Then the amount of GNP to provide the mass fractions of 1%, 3% and 5% was added into the molten A82. The liquid composite was mixed for 30 minutes with an ultrasonic mixing device of 750 W (Sonics & Materials INC, USA) as shown in Figure 2a to ensure the homogeneous distribution of the GNP nanoparticles inside the molten A82.

The dispersion capability of the nanoparticles within the A82 matrix was given by using the SEM (Tescan Mira 3 XMU, Czechia) images of the composite that doped with different sizes of GNP nanoparticles at 5% was given in Fig. 1. For the better visibility of the GNP network within the A82, only the SEM images of the composites having highest GNP mass fraction (%5) were given. It can be seen from Figure 1 that the lower size of nanoparticles (GNP 1-5nm) was made the agglomeration more favourable due to their sensitivity to fluid surface charges. It can be said that the possible network con not be occurred for the higher thermal conductivity, instead the over agglomeration acts negatively on it. On the other hand, it was observed that higher thickness nanoparticles (GNP 6-8 nm and GNP 11-15 nm) were found to be more uniformly dispersed within the A82. In these cases, it can be said that the surface charges are suitable for dispersion within the A82, therefore the agglomeration remains low. As a result, it can be said that an effective network is formed that will provide higher thermal conductivity enhancement.

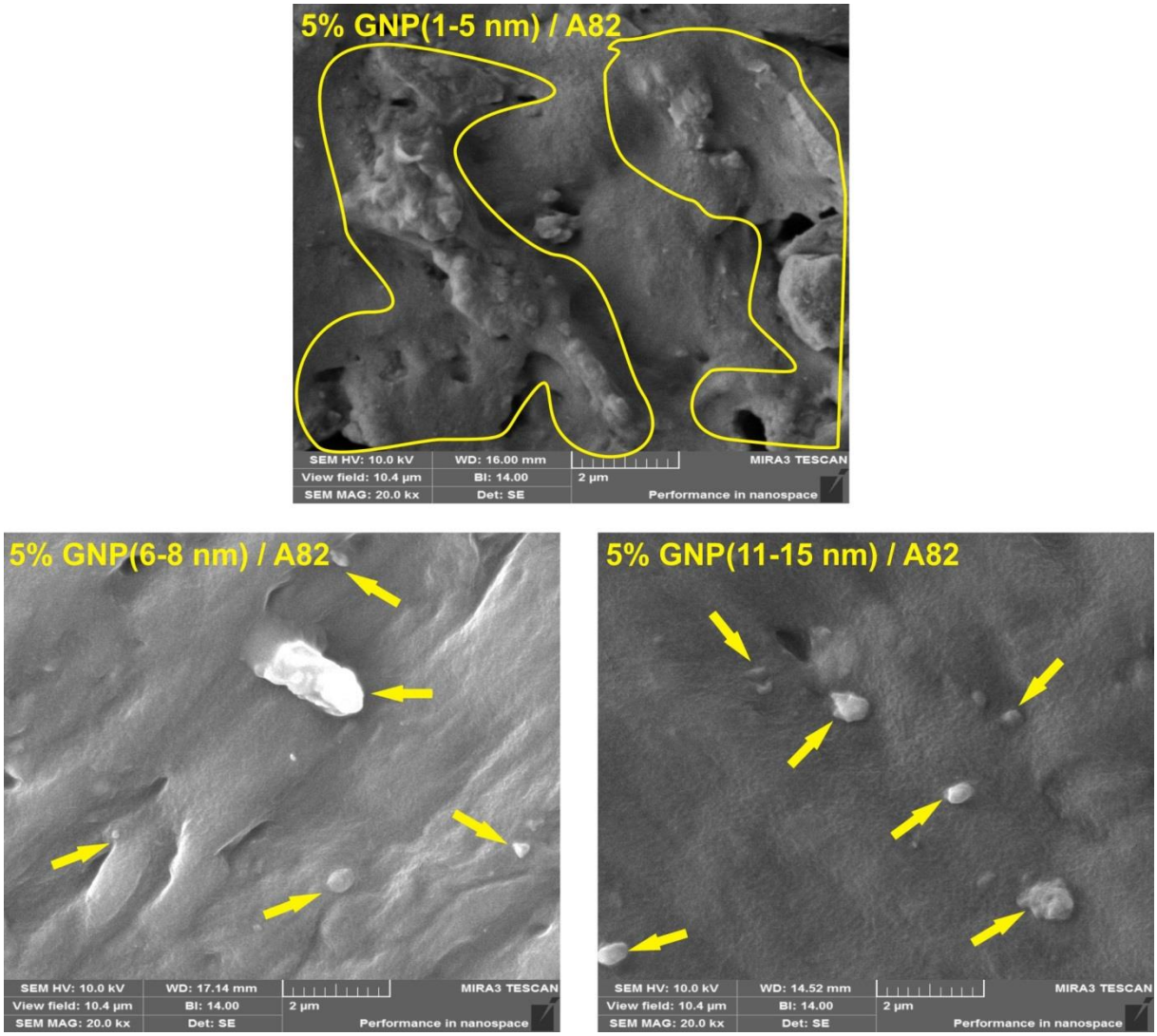

Figure 1. The SEM images of GNP/A82 composites

The thermal conductivities of the obtained homogeneous mixtures were measured with the KD2 Pro device (Decagon Devices Inc., USA), which operates in accordance with the principle of the transient linear heat

source. The KD2 Pro device consists of a microcontroller and a needle. The needle operates both as the heater and the temperature sensor and it determines the temperature change during the current throughout the heater in a time period. The thermal conductivity coefficient is determined as a result of the analysis of the measured temperatures for the same time period. The solid phase measurements were conducted with the TR1 sensor of the device (D=2.4mm, L=100mm) and the liquid phase measurements were conducted with the KS1 sensor (D=1.3mm, L=60mm). The measurement samples suitable to the KD2 Pro device need to be prepared in order to be able to measure the solid and liquid thermal conductivities of both the PCM and the GNP/A82 composites. The solid phase thermal conductivity measurement samples were prepared by pouring the obtained molten mixtures into a specially designed mold (Figure 2c) and solidifying them in room temperature (Figure 2d). As shown in Figure 2b, the solid phase sample mold consists of an acrylic cylinder with a diameter of 30 mm, a length of 120 mm and a pin in the middle with a diameter of 2.4 mm and a length of 100 mm. Therefore, the solid phase samples were obtained to allow sensor input in their axis. The liquid phase samples were carried out by placing the molten mixtures into a bottle with a diameter of 22 mm and a height of 75mm. Thermal conductivity measurements in different temperatures were conducted inside an air conditioner unit, each sample was measured at least five times and the mean values were given as the result. The measurement accuracy of the device in the solid phase is ± 10% for the range of 0.2-4 W/mK and ± 0.02 W/mK for the range of 0.1-0.2 W/mK. The liquid phase accuracy of the device is ±0.01 W/mK for 0.02-0.2 W/mK range.

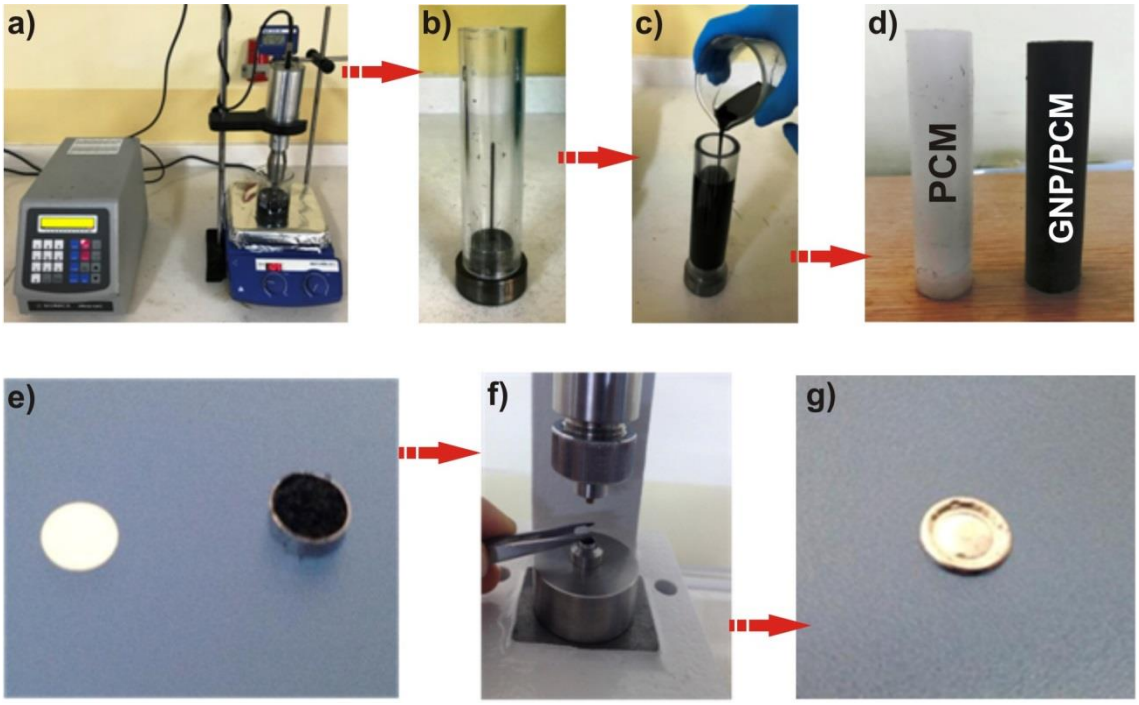

Figure 2. The preparation of the thermal conductivity and the DSC samples

The melting/solidification temperatures and the latent heats of the A82 or GNP/A82 composites were measured through the Differential Scanning Calorimetry (DSC) (DSC-60 Shimadzu Corporation, Japan) device. In order to prepare the DSC measurement samples, the dust particles extracted from the composites were weighed as about 5 mg using an electronic scale with a precision of 0.01 mg (Shimadzu Corporation, Japan). The DSC samples were prepared as a result of placing the weighed composite particles inside an aluminium container that is suitable to the device (Figure 2e) and pressing them together with the cover (Figure 2f) (Figure 2g). The DSC measurements were conducted within a temperature range of 20 ºC-120 ºC at a heating/cooling rate of 2 ºC/min. The measurements were conducted at least three times for each composite and the mean values were given as the result. The calorimetric precision and the temperature accuracy of the DSC device are ±1% and ±0.10 ºC.

The thermal performance measurements were carried out using the experimental setup shown in Figure 3. This setup consists of an energy storage unit, DC power supply, data acquisition device, computer, thermocouples and an air conditioner unit. The energy storage unit is an aluminium container with a diameter of 50 mm and a height of 100 mm, and an electrical resistance was placed to its cylinder axis as the heating supply.

The thermal performance of the A82 or GNP/A82 composites to be measured was poured into the energy storage unit in a liquid state and allowed to solidify for wrapping the electrical resistance. The electric resistance was operated through a DC power supply to dissipate 6W of heat. Thermal performance measurements were performed by measuring the thermal responses (temperatures) during the dissipation of heat released from the resistance in the energy storage unit along the A82 or GNP/A82. As shown in Figure 3, the thermal response measurements were conducted using the J-type thermocouples connected at half height to the outer surface of the resistance and the inner wall surface of the aluminium container. The temperature data were gathered in 30 second intervals through a data acquisition device and transferred to the computer. The energy storage unit was placed inside an air conditioner unit set at 20 ºC in order to ensure that all performance measurements are conducted under the same conditions.

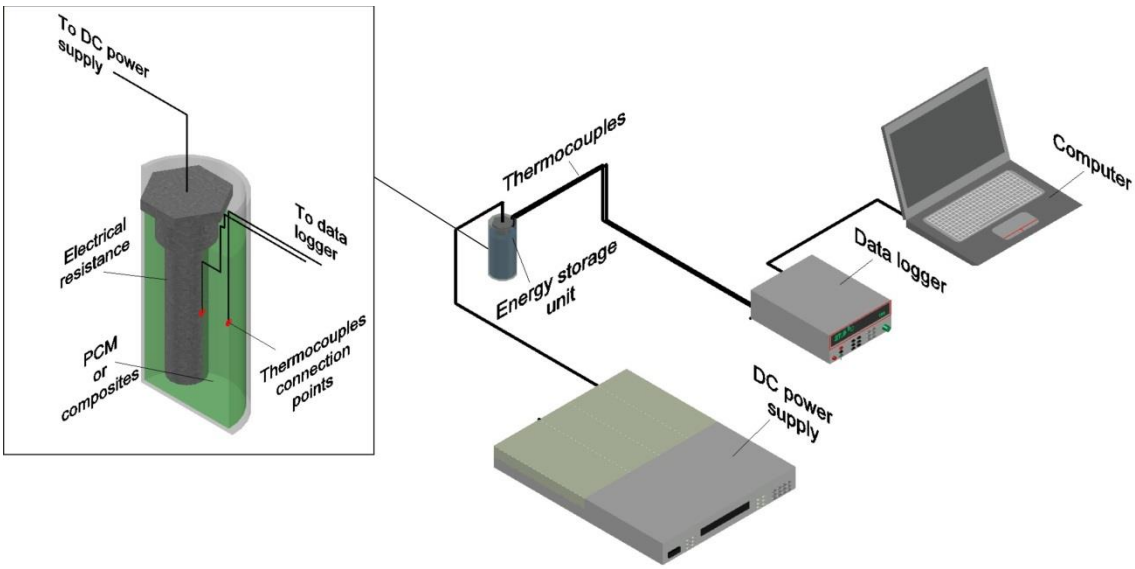

Figure 3. Experimental setup for thermal performance tests

III. RESULT AND DISCUSSION

Both the temperature dependent variation and percentage enhancement in thermal conductivity of the A82 composites which were doped with GNP in three different sizes (1-5nm, 6-8nm and 11-15nm) for the mass fractions of 1%, 3% and 5% were given in Figure 4. The measurements at 80 ºC could not be carried out as they coincided with the transition from solid to liquid. The following conclusions were deduced from the examination of Figure 4 at first sight. It was determined that both A82 and all composites obtained exhibited a decreasing trend in the solid phase state where the measurement temperature was less than 60 ºC. In addition, it was seen that the decreasing trend of thermal conductivity becomes more apparent based on the increase of the GNP mass fraction. The thermal conductivities of the A82 and GNP/A82 composites, which show decrease based on temperature, interestingly exhibit an unstable behaviour by slightly increasing at points close to the melting temperature (70 ºC). Similar results were observed in the MWCNTs composites, which were doped into a different organic PCM [21][16]. Thermal conductivities remain stable after a sharp decrease with the transition to liquid phase above 80 ºC. This situation is related to the conversion of more regular solid structure into irregular liquid structure.

It was seen from Figure 4 that the GNP nanoparticles with different thicknesses and surface areas caused different thermal enhancements on the thermal conductivities of the GNP/A82 composites. No apparent enhancement was observed in the thermal conductivity of the organic phase change material that was doped with the GNP with the largest surface area (750 m^2/g) and a thickness of 1-5 nm. On the contrary, deteriorations of up to 8% were detected in the thermal conductivities of the composites doped with 1% GNP (1-5nm). It can be said that these deteriorations occurred due to the over agglomeration or thermal resistance in the GNP-GNP and GNP-PCM interfaces. Thermal conduction in solid composites occurs through phonon transfer based on the lattice size of nano-materials and vibration frequency. It is clear that the GNP (1-5nm) thickness being low has a negative effect on phonon transfer. It can be said that in the case of a GNP (1-5nm) with a low thickness being doped into PCM in low mass fractions, thermal conductivity is low due to the fact that an efficient GNP network is not formed.

However, it is seen that thermal resistance deterioration began to be tolerated with the formation of the related conduction network based on increase in the GNP (1-5nm) mass fraction. This is also understood in the overlap of the thermal conductivity values of A82 and 3% GNP (1-5nm) / A82 composite. In the thermal conductivity of the A82 doped with 5% GNP (1-5nm), an average enhancement of 6.3% and 2.2% were provided for the solid phase and liquid phase respectively.

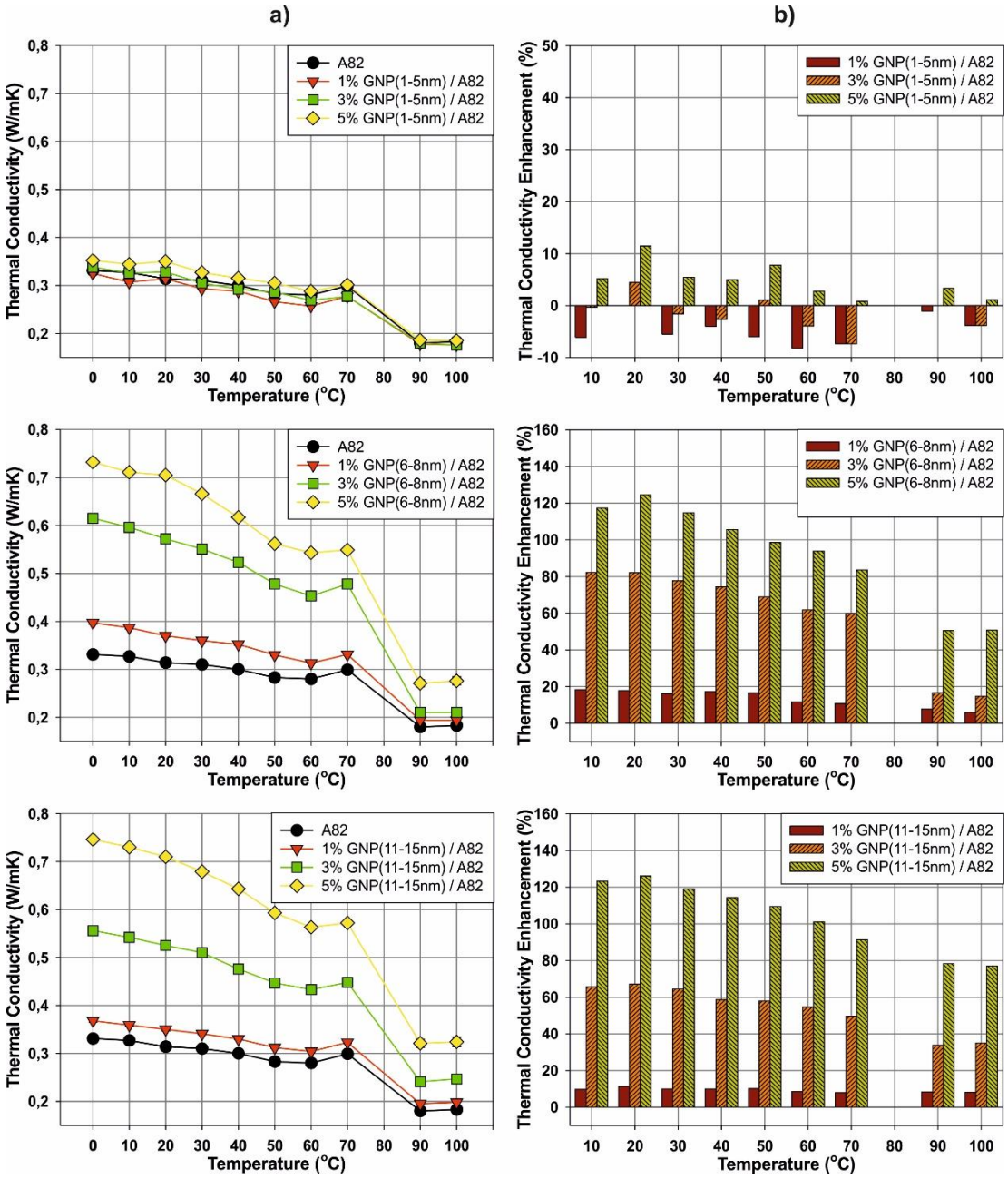

Figure 4. The effect of GNP size on thermal conductivity, a) thermal conductivity values, b) related enhancements in thermal conductivities

It was seen that GNP thickness increasing has a significant positive effect on the thermal conductivity enhancement although it decreases the nanoparticle surface area. On the other hand, it can be said that the thermal conductivity enhancement for the GNP/A82 composites at low mass fractions (1% and 3%) is a function of both GNP thickness and the surface area. In other words, while nanoparticle thickness increasing enhances the thermal conductivity, the surface area decreasing based on the increase in thickness has a negative effect on the thermal conductivity. For example, the average thermal conductivity enhancement of A82 doped with 1% GNP (6-8nm) having a thickness of 6-8 nm and a surface area of 120-150 m^2/g is 16.1% for the solid phase. On the other hand, the average thermal conductivity enhancement of A82 doped with 1% GNP (11-15nm) having a thickness of 11-

15nm and a surface area of 50-80 m^2/g is 9.9% for the solid phase. This situation is related to the fact that GNP (11-15nm) nanoparticles have a lower surface area compared to GNP (6-8nm) nanoparticles. Similar results are valid for the case of 3% GNP/A82 composites. Such that, average values of the solid phase thermal conductivity enhancements achieved for the 3% GNP (6-8nm)/A82 and 3% GNP (11-15nm)/A82 composites are 74.1% and 60.8% respectively. In summary, it can be said that the thermal conductivity enhancements in low mass fractions (1% and 3%) is a result of the optimization between GNP nanoparticle thickness and surface area. This situation is related to the fact that GNP (11-15nm), which has a lower surface area compared to GNP (6-8nm), causes higher thermal resistance in the GNP-PCM network. However, as the GNP (11-15nm) mass fraction is further increased, the negative thermal resistance effect was tolerated due to formation of more efficient conduction network by the nanoparticles with high thickness. In parallel with this result, the average solid phase thermal conductivity enhancements achieved for the 5% GNP (6-8nm)/A82 and 5% GNP (11-15nm)/A82 composites were determined as 107.5% and 113.7% respectively.

It can be said that, contrary to the solid phase thermal conductivities, the thermal conductivity enhancements in the liquid phase are independent of the GNP surface area but change in proportion with GNP thickness. In other words, the best thermal conductivity enhancements for the liquid A82 composites doped with GNPs in three different thicknesses were obtained by means of the addition of GNP (11-15nm). Such that, enhancements of 2.2%, 50.7% and 77.7% were achieved in the liquid phase average thermal conductivities of the A82 doped with 5% GNP (1-5nm), 5% GNP (6-8nm) and 5% GNP (11-15nm) respectively. Similar results are valid for the A82 composites doped with GNP in low mass fractions.

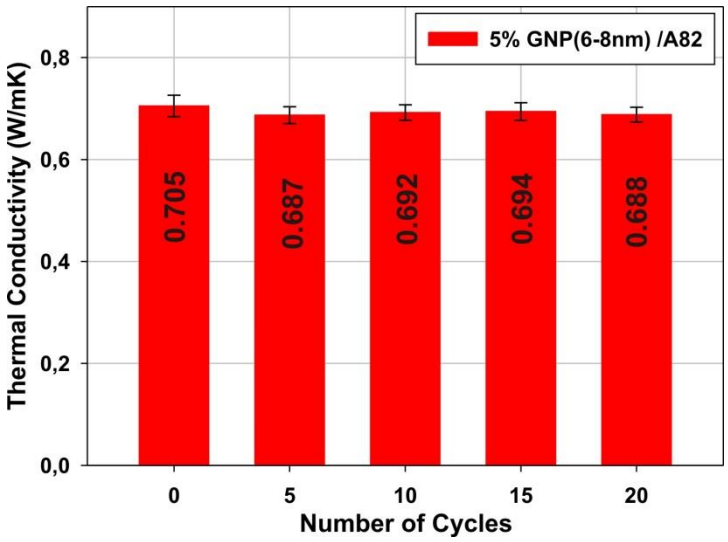

Figure 5. The thermal stability of the GNP/A82 composite

The sustainability or the stabilities of the thermal properties of GNP/A82 composites are an important issue. The reliable use of the composites in practice depends on the ability to maintain their thermal stability over a long term. The thermal stability tests were conducted by measuring the thermal conductivities of the 5% GNP (6-8nm)/A82 composite at the end of the melting/solidification cycles at an ambient temperature of 20 ºC. As can be seen from Figure 5, the variation in thermal conductivity throughout 20 heating/cooling cycles was less than 2.5%. This result is an indicator of the GNP (6-8nm)/A82 composite is thermally stable and thus that GNP nanoparticles maintain their homogeneous distribution within A82.

The effects of different sizes of GNP nanoparticles on melting/solidification temperatures and latent heats were given in Figure 6. It was determined that all of the thermogram curves given on the left side of Figure 6 exhibited similar behaviour. For example, it was seen that the endotherm curves related to melting occurs almost at the same temperature range and is independent from the GNP mass fraction and size. Similar results were seen for the exotherm curves related to solidification process. Quantitative DSC data regarding the melting and solidification phase change were obtained by analyzing the endotherm and exotherm curves and given on the right side of Figure 6. The melting peak temperature (T_{mp}) and solidification peak temperature (T_{sp}) for A82 were measured as 82.4 ºC and 80.5 ºC respectively and they were shown as a horizontal line in Figure 6b. The difference between T_{mp} and T_{sp} is known as the supercooling effect and the supercooling degree for A82 is 1.9 ºC. It was seen

that the change is less than 1 °C in the melting/solidification temperatures of the GNP/A82 composites doped with the GNP nanoparticle in different fractions and in different sizes. In this case, it can be said that the GNP mass fraction and/or GNP size has no effect on the melting/solidification temperatures.

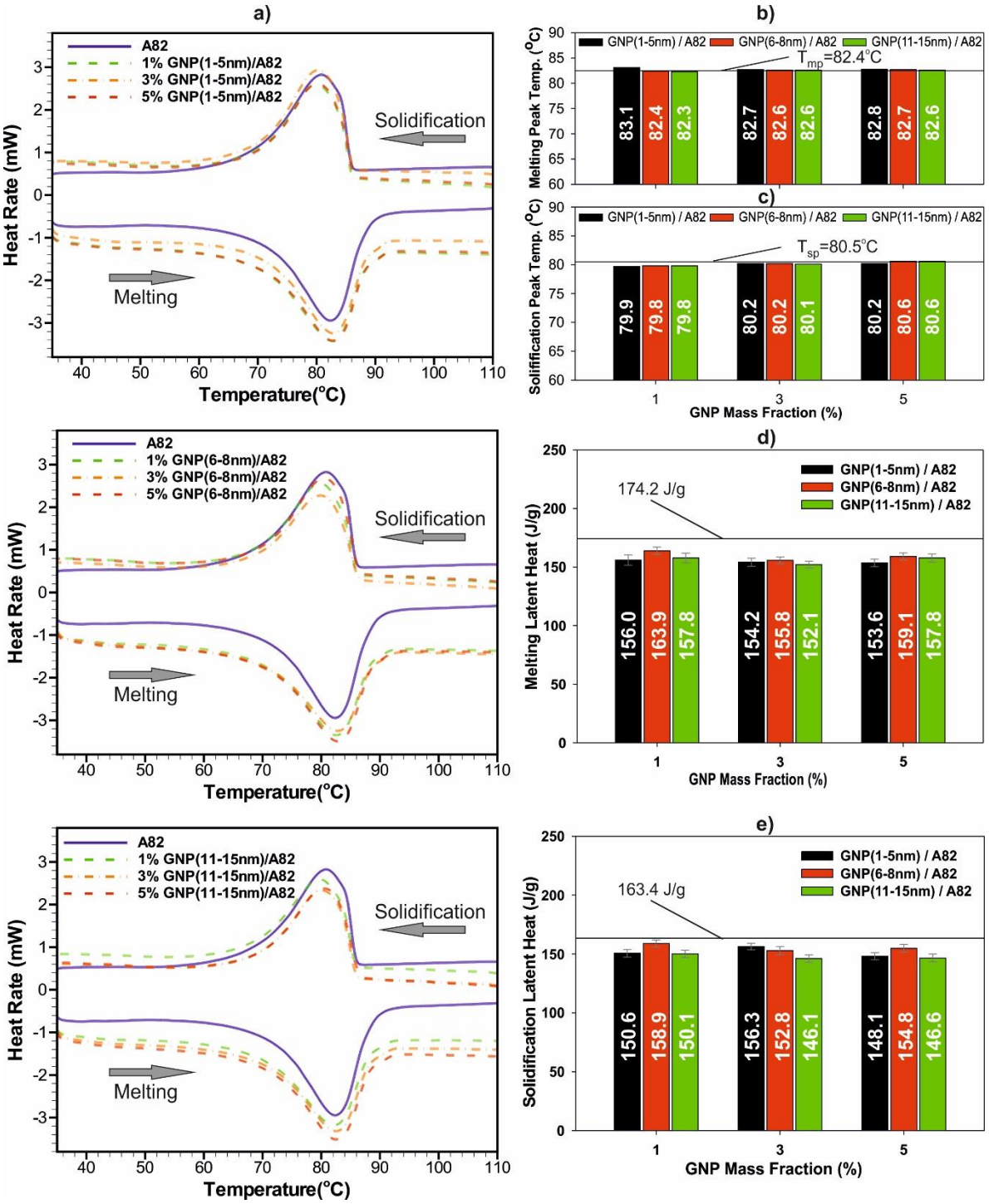

Figure 6. GNP size effect on DSC properties, a) DSC curves, b) Melting peak temperatures, c) Solidification peak temperatures, d) Melting latent heats, e) Solidification latent heats

Contrary to the melting/solidification temperatures of the GNP/A82 composites, the situation is different for their latent heats. Essentially the areas under the peaks curves of the endotherm and exotherm are related to the latent heat of melting and solidification respectively. The decreasing trend of the endotherm and exotherm peaks of the A82 composites, doped with in different size and mass fractions of GNP, is an indicator of decrease in their

melting/solidification latent heats. Theoretically, this is expected situation in adding the GNP nanoparticles with no energy storage capability into the A82. Essentially, their composite latent heat being decreased is related to the active A82 amount being decreased and the A82 being absorbed by GNP. The measured quantitative data of the melting/solidification latent heats were given in Figure 6. Primarily, it can be said that the melting and solidification latent heats of A82 are 174.2 J/g and 163.4 J/g respectively. The lower solidification latent heat compared to the melting latent heat is due to incomplete crystallization during solidification [22]. It was determined that the melting and solidification latent heats showed sharp decreases of up to 10.4% and 8.1% respectively in the case of GNP being doped into A82 in 1% mass fraction. In addition, it was determined that the GNP mass fraction being increased further did not affect the deterioration in latent heats significantly. Such that, the maximum deteriorations observed in the melting and solidification latent heats of the GNP/A82 composites were measured as 14.5% and 10.5% respectively compared to the melting and solidification latent heats of A82. In addition, no conclusion could be drawn about the size effect of GNP on the deteriorations of the melting and solidification latent heats.

The thermal performance tests of the GNP/A82 composites doped with GNP nanoparticles with different sizes were conducted by measuring their thermal responses (temperatures) from two different points. In Figure 7, time dependent variation of the temperature on the resistance was given for the composites A82, 5% GNP (1-5nm)/A82, 5% GNP (6-8nm)/A82 and 5% GNP (11-15nm)/A82. It is seen that initially, the temperature on the resistance is increased rapidly up to 50 ^{o}C. This situation is related to the fact that the sensible energy storage capacities of A82 and all other composites obtained are low. In this case, the temperature difference with the outer far field created by the increase of temperature on the resistance accelerates the heat transfer from the heat source to the outer region. Due to the aforementioned heat transfer, temperature increase on the resistance begins to decelerate from 50 ^{o}C. When the phase change begins about at 70 ^{o}C, the increase in temperature is distinctly limited due to the fact that A82 begins to store the heat generated by the resistance as latent energy. It can be said that the limitation in temperature increase is proportional to the enhancements achieved in the thermal conductivity of the GNP/A82 composite. This situation is related to the more effective dissipation of the heat generated by the resistance due to increased thermal conductivity. Thus, the temperature increase on the heat source remains lower.

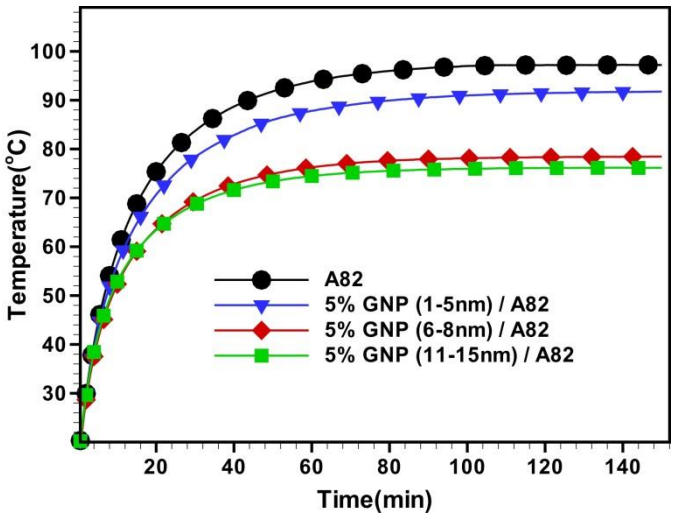

Figure 7. Thermal responses of heat source in using GNP/A82

In the case of the resistance wrapped with A82 being operated for 150 minutes, the average temperature on the resistance was measured as 88.7 ^{o}C. It was determined that the average temperature on the resistance decreased to 83.8 ^{o}C in the use of 5% GNP (1-5nm)/A82 composite. In that case thermal performance reflections were calculated according to the following equation.

$$\% \text{ performance} = \frac{T_{A82} - T_{com}}{T_{A82}} x100 \quad (1)$$

where;

T_{A82} : average temperature in using A82,

T_{com} : average temperature in using composite

It is clear that average of 6.3% enhancement in thermal conductivity is reflected to the thermal performance as 5.5% for the 5% GNP (1-5nm) / A82 composite. Similarly, in the performance tests conducted using 5% GNP (6-8nm)/A82 and 5% GNP (11-15)/A82, it was determined that the average temperatures on the resistance were 72.5 ºC and 71.0 ºC respectively. In parallel with the average enhancement of 107.5% achieved in thermal conductivity for the 5% GNP (6-8nm)/A82 composite, an enhancement of 18.3% was achieved in thermal performance. The best enhancement in thermal performance was achieved for the 5% GNP (11-15nm)/A82 composite. The thermal performance reflection of the 113.7% average enhancement achieved in thermal conductivity for the 5% GNP (11-15nm)/A82 composite was determined as 19.9%. It can be said that the reflection of the low thermal conductivity enhancements on performance is almost one to one. On the other hand, it is seen that the effect of the reflection to performance slows down significantly as the thermal conductivity enhancement increases.

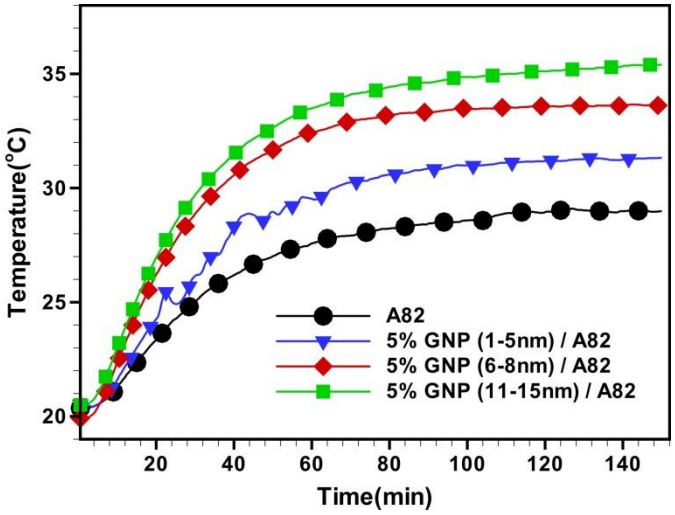

Figure 8. Thermal responses of container wall in using GNP/A82

Figure 8 shows the variation of temperature on the wall of the aluminium container over time for the composites A82, 5% GNP(1-5nm)/A82, 5% GNP(6-8nm)/A82 and 5% GNP(11-15nm)/A82. The average temperature on the wall for A82 was measured as 26.9 ºC. Contrary to the thermal response on the resistance, the temperature on the wall should be expected to increase in parallel with the increase in thermal conductivity. Because the heat generated from the resistance reach to the wall faster based on the thermal conductivity being increased. The average temperatures on the container wall were measured as 28.9 ºC, 31.1 ºC, 32.3 ºC respectively for the composites 5% GNP (1-5nm)/A82, 5% GNP (6-8nm)/A82 and 5% GNP (11-15 nm)/A82. The enhancements achieved in thermal performance compared to A82 were measured as 7.3%, 15.6% and 20% using the data of thermal response on the wall for the composites 5% GNP (1-5nm)/A82, 5% GNP (6-8nm)/A82 and 5% GNP (11-15nm)/A82 respectively. These results are compatible to the thermal performance enhancements measured over the resistance.

IV. CONCLUSIONS

In this study, the effect of GNP size on thermal properties such as thermal conductivity, melting/solidification temperatures and latent heat was examined. Also, the thermal performance reflections of the obtained thermal conductivity enhancements were determined.

At a low mass fraction of GNP, it was determined that the solid phase thermal conductivity enhancements were the functions of GNP nanoparticle thickness and the surface area. The best thermal conductivity enhancements in low mass fractions (1% and 3%) were obtained for GNP (6-8nm). The thermal conductivity enhancements of 1% GNP (6-8nm)/A82 and 3% GNP (6-8nm) /A82 composites were measured as 16.1% and 74.1% respectively. On the other hand, in the case of 5% GNP doped composites, the best thermal conductivity improvement was determined as 113.7% for the GNP (11-15nm) with the highest thickness. Similarly, it was determined that GNP (11-15nm) showed better results in the enhancement of liquid phase thermal conductivities

at all mass fractions. Regardless of the size, the doped GNP nanoparticles had no significant effect on melting/solidification temperatures, however, deteriorations of up to 14.5% and 10.5% were observed in the melting/solidification latent heats. It was determined that the rate of enhancement in thermal performance slowed down compared to the enhancement achieved in thermal conductivity. The reflection of the thermal conductivity enhancement of 113.7% achieved for the %5 GNP (11-15nm) composite to thermal performance was calculated as around 20%.

REFERENCES

[1] Liu, L., Su, D., Tang, Y., & Fang, G. (2016). Thermal conductivity enhancement of phase change materials for thermal energy storage: A review. *Renewable and Sustainable Energy Reviews*, *62*, 305–317. https://doi.org/10.1016/j.rser.2016.04.057

[2] Hadiya, J. P., & Shukla, A. K. N. (2016). Experimental thermal behavior response of paraffin wax as storage unit. *Journal of Thermal Analysis and Calorimetry*, *124(3)*, 1511–1518. https://doi.org/10.1007/s10973-016-5276-2

[3] Lorwanishpaisarn, N., Kasemsiri, P., Posi, P., & Chindaprasirt, P. (2017). Characterization of paraffin/ultrasonic-treated diatomite for use as phase change material in thermal energy storage of buildings. *Journal of Thermal Analysis and Calorimetry*, *128(3)*, 1293–1303. https://doi.org/10.1007/s10973-016-6024-3

[4] Zhou, D., Zhao, C. Y., & Tian, Y. (2012). Review on thermal energy storage with phase change materials (PCMs) in building applications. *Applied Energy*, *92*, 593–605. https://doi.org/10.1016/j.apenergy.2011.08.025

[5] Yuan, Y., Li, T., Zhang, N., Cao, X., & Yang, X. (2016). Investigation on thermal properties of capric–palmitic–stearic acid/activated carbon composite phase change materials for high-temperature cooling application. *Journal of Thermal Analysis and Calorimetry*, *124*, 881-888. https://doi.org/10.1007/s10973-015-5173-0

[6] Hallaj, S. Al, & Selman, J. R. (2000). A Novel Thermal Management System for Electric Vehicle Batteries Using Phase-Change Material. *Journal of The Electrochemical Society*, *147*, 3231-3236. https://doi.org/10.1149/1.1393888

[7] Khateeb, S. A., Farid, M. M., Selman, J. R., & Al-Hallaj, S. (2004). Design and simulation of a lithium-ion battery with a phase change material thermal management system for an electric scooter. *Journal of Power Sources*, *128*, 292-307. https://doi.org/10.1016/j.jpowsour.2003.09.070

[8] Hémery, C. V., Pra, F., Robin, J. F., & Marty, P. (2014). Experimental performances of a battery thermal management system using a phase change material. *Journal of Power Sources*, *270*, 349-358. https://doi.org/10.1016/j.jpowsour.2014.07.147

[9] Stritih, U. (2004). An experimental study of enhanced heat transfer in rectangular PCM thermal storage. *International Journal of Heat and Mass Transfer*, *47*, 2841-2847. https://doi.org/10.1016/j.ijheatmasstransfer.2004.02.001

[10] Agyenim, F., Eames, P., & Smyth, M. (2009). A comparison of heat transfer enhancement in a medium temperature thermal energy storage heat exchanger using fins. *Solar Energy*, 83, 1509-1520. https://doi.org/10.1016/j.solener.2009.04.007

[11] Xiao, M., Feng, B., & Gong, K. (2002). Preparation and performance of shape stabilized phase change thermal storage materials with high thermal conductivity. *Energy Conversion and Management*, *43*, 103-108. https://doi.org/10.1016/S0196-8904(01)00010-3

[12] Yang, J., Yang, L., Xu, C., & Du, X. (2016). Experimental study on enhancement of thermal energy storage with phase-change material. *Applied Energy*, *169*, 164-176. https://doi.org/10.1016/j.apenergy.2016.02.028

[13] Wang, J. F., Xie, H. Q., Li, Y., & Xin, Z. (2010). PW based phase change nanocomposites containing gamma-Al(2)O(3). *Journal of Thermal Analysis and Calorimetr*, *102*, 709-713. https://doi.org/DOI 10.1007/s10973-010-0850-5

[14] Ho, C. J., & Gao, J. Y. (2009). Preparation and thermophysical properties of nanoparticle-in-paraffin emulsion as phase change material. *International Communications in Heat and Mass Transfer, 36,* 467-470. https://doi.org/10.1016/j.icheatmasstransfer.2009.01.015

[15] Temel, Ü. N., & Çiftçi, B.Y. (2018). Determination of Thermal Properties of A82 Organic Phase Change Material Embedded with Different Type Nanoparticles. *Isı Bilimi ve Tekniği Dergisi* , 38, 75–85.

[16] Wang, J., Xie, H., Xin, Z., & Li, Y. (2010). Increasing the thermal conductivity of palmitic acid by the addition of carbon nanotubes. *Carbon, 48,* 3979-3986. https://doi.org/10.1016/j.carbon.2010.06.044

[17] Yu, Z. T., Fang, X., Fan, L. W., Wang, X., Xiao, Y. Q., Zeng, Y., … Cen, K. F. (2013). Increased thermal conductivity of liquid paraffin-based suspensions in the presence of carbon nano-additives of various sizes and shapes. *Carbon, 53,* 277-285. https://doi.org/10.1016/j.carbon.2012.10.059

[18] Fan, L. W., Fang, X., Wang, X., Zeng, Y., Xiao, Y. Q., Yu, Z. T., … Cen, K. F. (2013). Effects of various carbon nanofillers on the thermal conductivity and energy storage properties of paraffin-based nanocomposite phase change materials. *Applied Energy, 110,* 163-172. https://doi.org/10.1016/j.apenergy.2013.04.043

[19] Cui, Y., Liu, C., Hu, S., & Yu, X. (2011). The experimental exploration of carbon nanofiber and carbon nanotube additives on thermal behavior of phase change materials. *Solar Energy Materials and Solar Cells, 51,* 365-372. https://doi.org/10.1016/j.solmat.2011.01.021

[20] Shi, J. N., Ger, M. Der, Liu, Y. M., Fan, Y. C., Wen, N. T., Lin, C. K., & Pu, N. W. (2013). Improving the thermal conductivity and shape-stabilization of phase change materials using nanographite additives. *Carbon, 51,* 365-372. https://doi.org/10.1016/j.carbon.2012.08.068

[21] Wang, J., Xie, H., & Xin, Z. (2009). Thermal properties of paraffin based composites containing multi-walled carbon nanotubes. *Thermochimica Acta, 488,* 39-42. https://doi.org/10.1016/j.tca.2009.01.022

[22] Wang, J., Xie, H., Xin, Z., Li, Y., & Chen, L. (2010). Enhancing thermal conductivity of palmitic acid based phase change materials with carbon nanotubes as fillers. *Solar Energy, 84,* 339-344. https://doi.org/10.1016/j.solener.2009.12.004